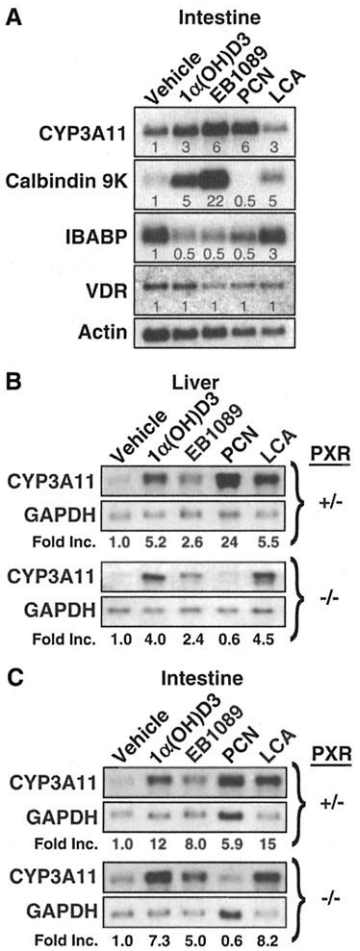

Fig. 4. LCA activation of VDR target genes in vivo. (**A**) Regulation of VDR, PXR, and FXR target gene expression in small intestine. Mice were treated with the indicated ligands or vehicle (corn oil) for 3 days, and small intestine was harvested for Northern blot (RNA) analysis (*25*) using 5 μg pooled mRNA (n = 6 animals). (**B** and **C**) Regulation of CYP3A11 expression in liver and intestine of $PXR^{-/-}$ and $PXR^{+/-}$ mice. Northern blot analysis was performed on liver of mice treated as in (A). Representatives of three independent experiments are shown. The numbers under the lanes indicate fold increases in expression relative to the vehicle and were standardized against actin or glyceraldehyde phosphate dehydrogenase (GAPDH) controls. 1αD3,1α-hydroxy-vitamin D_3.

17. Z. Araya, K. Wikvall, *Biochim. Biophys. Acta* **1438**, 47 (1999).
18. M. R. Haussler *et al.*, *J. Bone Miner. Res.* **13**, 325 (1998).
19. S. A. Kliewer *et al.*, *Cell* **92**, 73 (1998).
20. A. M. Kissmeyer *et al.*, *Biochem. Pharmacol.* **53**, 1087 (1997).
21. A. Chawla, J. J. Repa, R. M. Evans, D. J. Mangelsdorf, *Science* **294**, 1866 (2001).
22. M. Lipkin, B. Reddy, H. Newmark, S. A. Lamprecht, *Annu. Rev. Nutr.* **19**, 545 (1999).
23. E. Kallay *et al.*, *Carcinogenesis* **22**, 1429 (2001).
24. T. T. Lu *et al.*, *Mol. Cell* **6**, 507 (2000).
25. Male mice (129Sv wild type, $PXR^{+/-}$, or $PXR^{-/-}$) were gavaged daily with vehicle (corn oil), 1.5 μg $1\alpha(OH)D_3$ (gift from M. Pechet, Research Institute for Medicine and Chemistry, Cambridge, MA), 1.5 μg EB1089 (gift from L. Binderup, Leo Pharmaceutical Products, Copenhagen), 1.5 mg PCN, or 8 mg LCA. Mice were killed, and mRNA from the intestine and liver were isolated for Northern blot analysis (*24*) using the indicated gene-specific cDNA probes.
26. We thank J. Repa, K. Gauthier, and N. Kalaany for assistance in animal experiments; C. Wu and A. Kowal for expert technical assistance; C. Haussler and members of the Mango lab for comments; and M. Brown, J. Goldstein, and D. W. Russell for critically reading the manuscript. D.J.M. and R.M.E. are investigators and M.M. is an associate of the Howard Hughes Medical Institute. T.T.L. is supported by a Pharmacological Sciences training grant from NIH. Funded by the Howard Hughes Medical Institute, an NIH Specialized Program of Research Excellence in lung cancer, the Robert A. Welch Foundation, the Human Frontier Science Program, and NIH grants (M.R.H.).

Supporting Online Material
(www.sciencemag.org/cgi/content/full/296/5571/1313/DC1)
Material and Methods
fig. S1

1 February 2002; accepted 4 April 2002

Heterotopic Shift of Epithelial-Mesenchymal Interactions in Vertebrate Jaw Evolution

Yasuyo Shigetani,[1]* Fumiaki Sugahara,[2] Yayoi Kawakami,[2] Yasunori Murakami,[1] Shigeki Hirano,[3] Shigeru Kuratani[1,2]†

Genes involved in late specification of the mandibular arch, the source of the vertebrate jaw, are expressed with similar patterns in the oral regions of chick and lamprey embryos. However, morphological comparisons indicate that apparently orthologous homeobox genes were expressed in different subdivisions of the ectomesenchyme in the two species. Therefore, the homology and gene expression of the oral region are uncoupled during the transition from agnathan to gnathostome; we conclude that a heterotopic shift of tissue interaction was involved in the evolution of the jaw.

Conventional comparative anatomy assumes that the vertebrate jaw was acquired through modification of the mandibular arch, the most rostral element of the pharyngeal arches (Fig. 1A): In primitive vertebrates, the arches resembled one another, showing no specialization. The mandibular arch was then dorsoventrally subdivided and enlarged to differentiate the upper and lower jaw cartilages (Fig. 1A, right). However, the larval oral apparatus in the lamprey, a jawless vertebrate (agnathan), exhibits well-differentiated upper and lower lips for which morphologic homologies (*1*) with the jaws are not certain (*2*) (Fig. 1B). Moreover, the early embryonic pattern of the lamprey is very similar to that of the jawed vertebrates (gnathostomes): Homologous patterns are seen in the global deployment of crest cells (*3*), in the configuration of the mesoderm (*4*), and even in the expression of some regulatory genes, including *Otx*, a gene involved in gnathostome jaw development (*5*, *6*).

During development of the amniote mandibular arch, *Dlx* and *Msx* homeobox genes are expressed in an overlapping fashion in the crest-derived ectomesenchyme, and they prefigure the proximal-distal axis of the mandibular arch (Fig. 1C) (*7*, *8*). These genes are regulated through epithelial-mesenchymal interactions (*9*), downstream of growth factors secreted by the epidermis (*7*, *8*). In the chick late pharyngula, a growth factor–encoding gene, *cFgf8*, is expressed in the perioral epidermis (Fig. 1D), and its target gene, *cDlx1*, is expressed in the subadjacent ectomesenchyme (Fig. 1E) (*10*). Another growth factor, *cBmp4*, is expressed in the distal epidermis of the upper and lower jaws (Fig. 1F); its downstream gene, *cMsx1*, is expressed in the distal ectomesenchyme (Fig. 1G).

We isolated the above gene cognates from a cDNA library of the Japanese lamprey, *Lampetra japonica*, and observed their expression patterns in the embryonic oral region. Molecular phylogenetic analyses have indicated that the isolated genes,

[1]Laboratory for Evolutionary Morphology, Center for Developmental Biology, RIKEN, Hyogo 650-0047, Japan. [2]Department of Biology, Okayama University, Okayama 700-8530, Japan. [3]Department of Medical Technology, Niigata University, Niigata 951-8518, Japan.

*Present address: Division of Developmental Neurobiology, National Institute for Medical Research, Mill Hill, London NW7 1AA, UK.

†To whom correspondence should be addressed. E-mail: saizo@cdb.riken.go.jp

termed *LjFgf8/17* (designated *Lj* for *Lampetra japonica*), *LjDlx1/6* (*11*), *LjBmp2/4a*, and *LjMsxA*, correspond to the above-listed gnathostome genes (*12*). In situ hybridization (*10*) showed that *LjFgf8/17* was expressed in the perioral epidermis (Fig. 1H), *LjDlx1/6* was expressed in the ectomesenchyme subadjacent to the *LjFgf8/17*-expressing epidermis (Fig. 1I), *LjBmp2/4a* was expressed in the distal epidermis of the upper and lower lips (Fig. 1J), and *LjMsxA* was expressed in the mesenchyme subadjacent to *LjBmp2/4a*- expressing epidermis (Fig. 1K).

To determine whether the above gene expression patterns were based on conserved signaling cascades, we applied FGF8 and BMP4 proteins ectopically to early lamprey embryos. We showed that both proteins were able to up-regulate the endogenous lamprey putative target genes (Fig. 1, L and M) (*13*). Thus, the molecular cascades of the growth factors and their target homeobox genes are likely to be conserved between lampreys and gnathostomes. Furthermore, *LjDlx1/6* and *LjMsxA* are likely to be up-regulated through epithelial-mesenchymal interactions as in amniote embryos.

The above findings appear to support morphological homologies between lamprey larval lips and gnathostome jaws. To substantiate this, we labeled the premigratory neural crest of lamprey embryos with the lipophilic dye 1,1-dioctadecyl-3,3,3′,3′-tetramethylindocarbocyanine perchlorate (DiI, Molecular Probes, Eugene, OR) to map the origins of the oral ectomesenchyme (*14*). We found that the upper and lower lip–forming crest cells were derived from the forebrain to hindbrain areas (Fig. 2) more extensively than those in the gnathostome mandibular arch (*15*). In particular, the upper lip cells were derived mostly from the forebrain and rostral midbrain (Fig. 2, A and C), like the premandibular region of amniotes (*15–17*). Thus, the distribution of the ectomesenchyme is not simply comparable between the lamprey and gnathostomes based on the crest cell origins, and neural crest mapping is insufficient to establish homology of crest cell subpopulations. Rather, morphological analysis should reveal topographical relationships of cell populations, which form the basis for embryonic induction (*1*).

As discussed previously (*2*), three topographically comparable regions can be recognized in the rostral ectomesenchyme of the lamprey and gnathostome embryos: namely, the nasal, postoptic, and mandibular regions. These are not arbitrary divisions, because each ectomesenchymal region is associated with distinct, shared embryonic structures (Fig. 3, A and B). The upper lip in the lamprey is a postoptic derivative that lies lateral to the premandibular mesoderm (Fig.

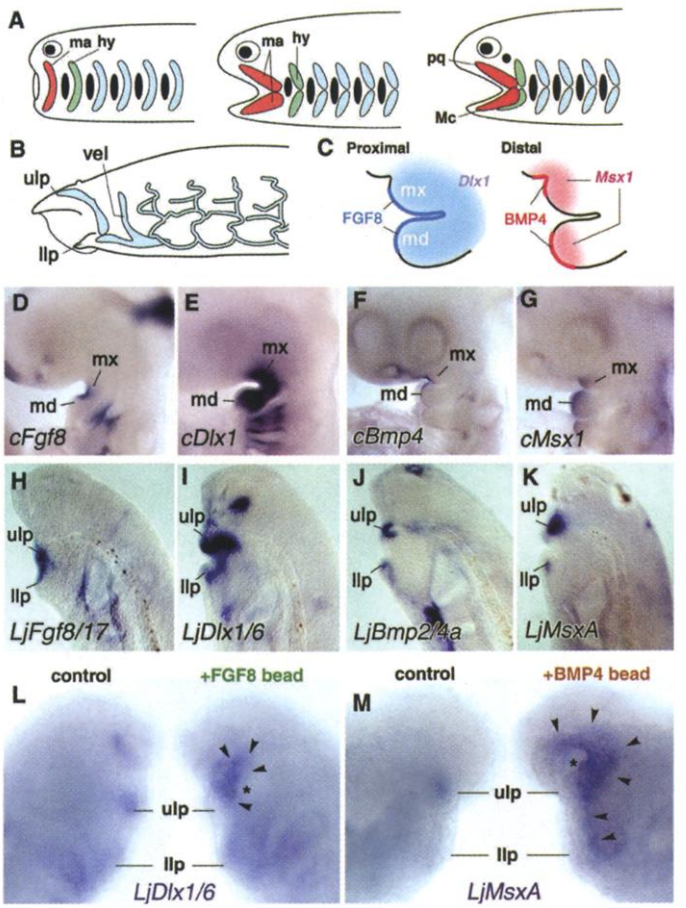

Fig. 1. Jaw evolution and functions of signaling molecules in the mandibular arch. (**A**) Hypothetical evolutionary transition of the jaw. The first two pharyngeal arches [mandibular (ma) and hyoid (hy) arches] are labeled. Although the arches resemble each other in the ancestral condition, the mandibular arch is enlarged toward gnathostomes (right). Finally, palatoquadrate (pq) and Meckel's (Mc) cartilages differentiate in the upper and lower jaw, respectively. (**B**) The oral structure of the larval lamprey is composed of upper (ulp) and lower (llp) lips and a velum (vel). (**C**) Expression patterns of proximal and distal genes are diagrammatically indicated in the gnathostome mandibular arch. (**D** to **G**) Expression patterns of jaw-patterning genes in the chick embryo. (**H** to **K**) Expression patterns of homologous genes in the lamprey embryo. (**L** and **M**) Ectopic application of growth factors (asterisks) induced ectopic up-regulation of putative target genes (arrowheads) in the lamprey embryo. The left side of each image shows the intact control side of the same embryo.

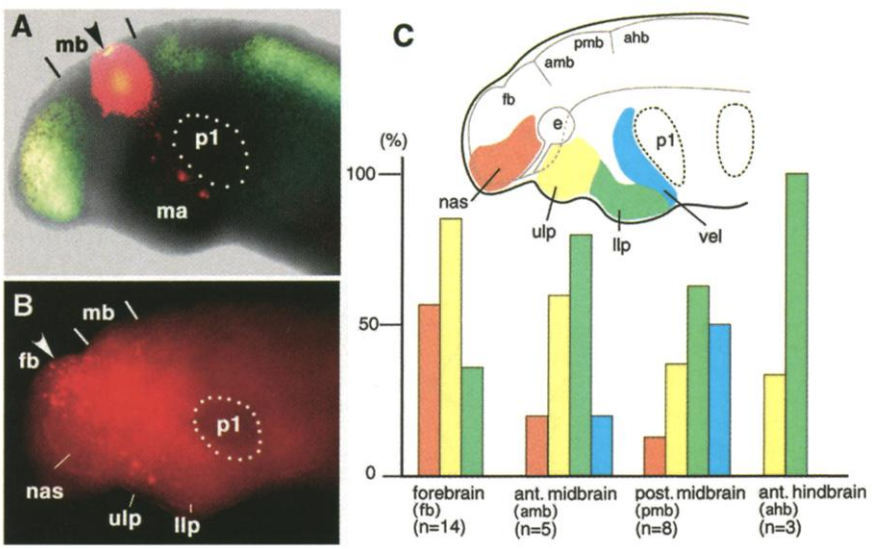

Fig. 2. Origin of the oral ectomesenchyme. (**A**) DiI was injected into the posterior midbrain (arrowhead) of the lamprey neurula. At early pharyngula, most of the labeled cells populated the mandibular arch (ma). The expression pattern of *LjPax6* in another embryo at the same stage is superimposed in green. The midbrain (mb) is devoid of *LjPax6* transcripts (*25*). p1, pharyngeal pouch 1. (**B**) DiI was injected in the forebrain (fb; arrowhead). Some labeled cells populated the nasal region (nas) as well as the upper (ulp) and lower (llp) lips. (**C**) (Top) Schematic illustration of the lamprey embryo, in which rostral ectomesenchyme is subdivided into four regions. (Bottom) Bar graph shows ratio of embryos with labeled cells in each region. Bars are colored according to subdivisions shown in the above scheme. e, eye; vel, velar region.

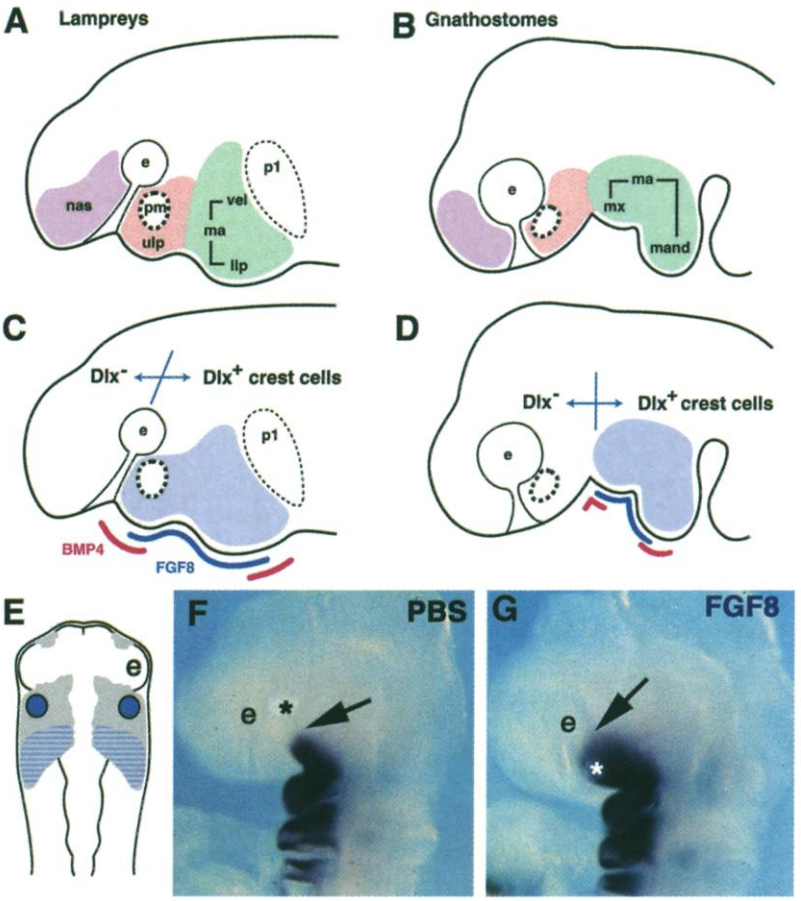

Fig. 3. Comparative morphology of the rostral ectomesenchyme. (**A** and **B**) In both the lamprey and gnathostomes, the rostral ectomesenchyme is divided into nasal (purple), postoptic (pink), and mandibular (green) regions (*2*). Postoptic cells surround the premandibular mesoderm (pm). In the lamprey (A), the lower lip (llp) and velum (vel) are derived from the mandibular crest cells, whereas the upper lip (ulp) is of postoptic origin. In gnathostomes (B), the mandibular arch (ma) differentiates into the maxillary (mx) and mandibular (mand) processes. e, eye; p1, pharyngeal pouch 1. (**C** and **D**) Gene expression patterns are not consistent with the ectomesenchymal morphology. The *Dlx1/6* gene (light blue) is expressed in the entire mesenchyme caudal to the eye in the lamprey (C) but only in the mandibular arch in the gnathostome embryo (D). This difference of gene expression corresponds to the distribution of growth factors in the epidermis (blue, FGF8; red, BMP4). (**E**) FGF8-soaked beads (blue circles) were implanted in the postoptic region of stage 9 chick embryos. (**F** and **G**) *cDlx1* expression after 24 hours of bead implantation (asterisk). The rostral limit of *cDlx1* expression was shifted rostrally (arrow) in the experimental embryo (G) compared with the control (F), which received PBS-soaked beads.

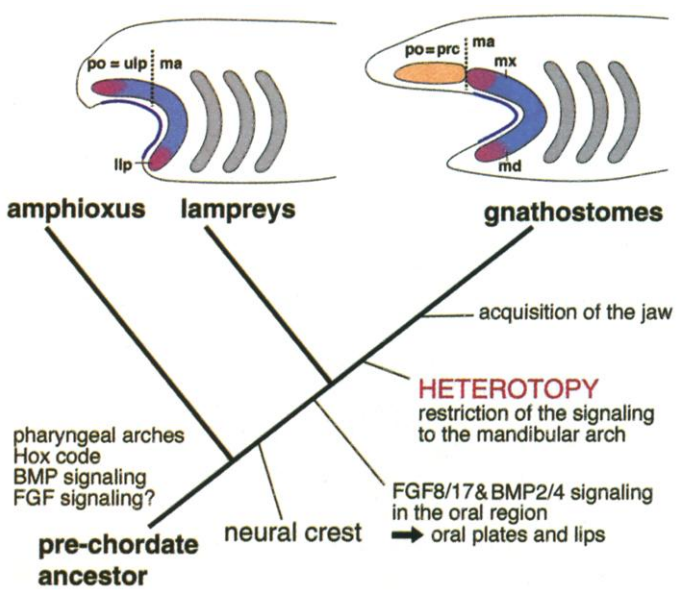

Fig. 4. A scenario for jaw evolution. (**Top**) Patterning of crest cells is compared between lampreys and gnathostomes. In both the animals, the ectomesenchyme contains postoptic (po) and mandibular arch (ma) subdomains. Growth factors secreted by the epidermis (blue line) induce target homeobox genes (pink and blue) in the entire lamprey ectomesenchyme, whereas in gnathostomes the same signaling is effective only in the mandibular component. Thus, the phenotypically similar protrusions originate from nonequivalent cell populations in the two animals. Heterotopic shift of epithelial-mesenchymal interactions is assumed to be behind this difference. The postoptic crest cells occupy the site of prechordal cranium (prc) in gnathostomes. Broken lines indicate the boundary between postoptic (po) and mandibular (ma) ectomesenchyme. (**Bottom**) The evolutionary sequence of the changes in developmental patterning is summarized on the phylogenetic tree. The vertebrate ancestor had acquired neural crest–derived ectomesenchyme after the split from amphioxus, as an element for epithelial-mesenchymal interactions. The molecular cascades for the interactions may have already been present in the ancestral vertebrates. Although these genes may have already been involved in oral patterning in agnathans, a heterotopic shift must be assumed in the lineage leading to gnathostomes to explain the topographic discrepancy shown at top.

3, A and B) (*2*). The equivalent ectomesenchymal portion in gnathostomes corresponds to the site of prechordal cranium (*18*) and not to the upper jaw (*2*). Thus, the oral region in the lamprey is most probably a composite of the mandibular arch and postoptic ectomesenchyme, and the morphological homology between the upper lip and upper jaw is unlikely (*2*). This also leads to the conclusion that the *Dlx1* cognates are expressed in different parts of the ectomesenchyme between the lamprey and gnathostomes (Fig. 3, C and D). This difference in spatial gene expression patterns may be due to the varied distribution of the FGF8 molecules in the epidermis (Fig. 3, C and D). Actually, by applying the FGF8 recombinant protein to the postoptic region of the chick embryo (Fig. 3E) (*15*), we obtained a lamprey-like expression pattern of *cDlx1* in the experimental embryo (compare Fig. 3G with Fig. 3F).

We hypothesize that the origin of neural crest–derived ectomesenchyme in a vertebrate ancestor resulted in the increased importance of growth factor–mediated tissue interactions (*19*). FGF8/17- and BMP2/4-mediated molecular cascades would have already been functional in the ancestral animal. The shared molecular cascades for oral patterning between lampreys and gnathostomes imply that a part of the developmental mech-

anism that shapes oral protrusions (jaws and lips) preceded evolution of jaws (Fig. 4). In some of the Paleozoic agnathans, movable oral plates and lips are thought to be very similar to jaws at the phenotypic level (*20*). However, there are no morphologic homologies (*1*) between jaws and lips that can satisfy both the gene expression patterns and the topographic relationships of the structures simultaneously. Rather, the shared molecular mechanisms are regarded as exaptations (*21*) for jaw evolution and not as a guide for homology. We conclude that a topographical shift of epithelial-mesenchymal interaction lies behind this difference.

As inferred by the present study, the difference in developmental patterning may partly be due to the caudal restriction of growth factors in the epidermis (Fig. 4, top). Haeckel (*22*) has defined such a change in the place of development as "heterotopy." In organisms such as vertebrates, in which epigenetic tissue interaction plays an essential role in morphogenetic patterning, the shift of epigenetic interactions alters the regulatory gene expression patterns in the mesenchyme (*9*), which leads to reorganization of tissue morphological identities. Thus, the gene cascades and morphological homology are uncoupled through the process of heterotopy. In this sense, the gnathostome jaw is truly an evolutionary innovation, which appears to have been obtained by overcoming ancestral developmental constraints (*23*). What brought about this shift in the regulation of the growth factor–encoding genes requires future study.

References and Notes

1. G. P. Wagner, in *Homology: The Hierarchical Basis of Comparative Biology*, B. K. Hall, Ed. (Academic Press, San Diego, CA, 1994), pp. 273–299.
2. S. Kuratani, Y. Nobusada, N. Horigome, Y. Shigetani, *Philos. Trans. R. Soc. London* **356**, 15 (2001).
3. N. Horigome *et al.*, *Dev. Biol.* **207**, 287 (1999).
4. S. Kuratani, N. Horigome, S. Hirano, *Dev. Biol.* **210**, 381 (1999).
5. T. Ueki, S. Kuratani, S. Hirano, S. Aizawa, *Dev. Genes Evol.* **208**, 223 (1998).
6. I. Matsuo, S. Kuratani, C. Kimura, N. Takeda, S. Aizawa, *Genes Dev.* **9**, 2646 (1995).
7. A. Neubüser, H. Peters, R. Ballin, G. R. Martin, *Cell* **90**, 247 (1997).
8. C. A. Ferguson, A. S. Tucker, P. T. Sharpe, *Development* **127**, 403 (2000).
9. B. K. Hall, *Evolutionary Developmental Biology* (Chapman & Hall, London, ed. 2, 1998).
10. Whole-mount in situ hybridization of chick and lamprey embryos was carried out as described in (*24*).
11. M. Myojin *et al.*, *Mech. Dev. Evol.* **291**, 58 (2001)
12. Details of the *LjFgf8/17*, *LjBmp2/4a*, and *LjMsxA* sequences of *L. japonica* have been deposited in GenBank under accession numbers AB071892, AB071890, and AB072037, respectively. Phylogenetic analyses of these genes are available as supporting online material.
13. Heparin beads (Sigma) soaked with mouse FGF8b (500 μg/ml; R&D Systems, Minneapolis, MN) and human BMP4 (500 μg/ml; R&D Systems) were implanted in the embryonic lamprey head. After 2 days, the embryos were fixed with 4% paraformaldehyde (PFA) in phosphate-buffered saline (PBS). For the chick embryo, the same recombinant beads were implanted in both sides of the postoptic region of seven-somite embryos.
14. Embryos of *L. japonica* were injected with a solution of DiI (Molecular Probes, Eugene, OR) as described in (*3*). Embryos were then incubated 24 to 48 hours and fixed with 2% PFA containing 1.25% glutaraldehyde in PBS and then cleared with 80% glycerol for observation by fluorescence microscopy.
15. Y. Shigetani, Y. Nobusada, S. Kuratani, *Dev. Biol.* **228**, 73 (2000).
16. N. Osumi-Yamashita, Y. Ninomiya, H. Doi, K. Eto, *Dev. Biol.* **126**, 409 (1994).
17. G. Köntges, A. Lumsden, *Development* **122**, 3229 (1996).
18. F. C. Couly, P. M. Colty, N. M. Le Douarin, *Development* **117**, 409 (1993).
19. C. Gans, R. G. Northcutt, *Science* **220**, 268 (1983).
20. P. Janvier, *Early Vertebrates* (Oxford Scientific, New York, 1996).
21. S. J. Gould, E. S. Vrba, *Paleobiology* **8**, 4 (1982).
22. E. Haeckel, *Jena Z. Naturwiss.* **9**, 402 (1875).
23. G. B. Müller, G. P. Wagner, *Annu. Rev. Ecol. Syst.* **22**, 229 (1991).
24. M. Ogasawara, Y. Shigetani, S. Hirano, N. Satoh, S. Kuratani, *Dev. Biol.* **223**, 399 (2000).
25. Y. Murakami *et al.*, *Development* **128**, 3521 (2001).

26. We thank P. Holland for critical reading of the manuscript, I. Araki for the *cFgf8* cDNA probe, K. Shimamura and J. Rubenstein for the *cDlx1* cDNA probe, T. Nohno for *cBmp4* and *cMsx1* cDNA probes, and S. Kuraku and T. Miyata for phylogenetic analyses of lamprey genes. Supported by grants-in-aid from the Ministry of Education, Science and Culture of Japan to S.K.

Supporting Online Material

(www.sciencemag.org/cgi/content/full/296/5571/1316/DC1)
fig. S1

26 November 2001; accepted 4 April 2002

Induction and Suppression of RNA Silencing by an Animal Virus

Hongwei Li, Wan Xiang Li, Shou Wei Ding*

RNA silencing is a sequence-specific RNA degradation mechanism that is operational in plants and animals. Here, we show that flock house virus (FHV) is both an initiator and a target of RNA silencing in *Drosophila* host cells and that FHV infection requires suppression of RNA silencing by an FHV-encoded protein, B2. These findings establish RNA silencing as an adaptive antiviral defense in animal cells. B2 also inhibits RNA silencing in transgenic plants, providing evidence for a conserved RNA silencing pathway in the plant and animal kingdoms.

Posttranscriptional gene silencing, quelling, and RNA interference (RNAi) are mechanistically related RNA silencing processes that destroy RNA in a sequence-specific manner (*1*, *2*). Available data show that double-stranded RNA (dsRNA) serves as the initial trigger of RNA silencing and, after recognition, is processed by the Dicer RNase into short fragments of 21 nucleotides (nt) in length. These short interfering RNAs (siRNAs) are then incorporated into a dsRNA-induced silencing complex (RISC) to guide cycles of specific RNA degradation (*1*, *2*). Here, we report that RNA silencing plays a natural antiviral role in animal cells, as has been established in plants (*3*, *4*).

We focused on the flock house virus (FHV) because its *B2* gene (see fig. S1) shares key features, but not sequence similarity, with the plant cucumoviral *2b* gene (*5*), which encodes a known group of silencing suppressors (*6*, *7*). Both open reading frame (ORF) 2b and B2 overlap the carboxyl terminal region and occupy the +1 reading frame of the ORF encoding the viral RNA-dependent RNA polymerase and are translated in vivo by a subgenomic mRNA (*5*).

The FHV B2 protein indeed exhibited a potent silencing-suppression activity (Fig. 1) in the *Agrobacterium* co-infiltration assay (*8*), established in transgenic plants that express green fluorescent protein (GFP). Transient B2 expression prevented RNA silencing of the GFP transgene, leading to a strong and prolonged green fluorescence examined under ultraviolet (UV) illumination (Fig. 1, left), similar to suppression by the cucumoviral 2b proteins (*9*) (Fig. 1, right). In contrast, a broad red fluorescent zone surrounding the infiltrated patch (Fig. 1, middle) became clearly visible 6 days after infiltration, when the co-infiltrated transgene directed translation of neither 2b nor B2.

RNA blot hybridizations confirmed that expression of either protein was associated with high accumulation levels of the GFP mRNA (see fig. S2). In addition, the GFP-specific siRNAs, a hallmark of RNA silencing (*10*), remained at extremely low levels in the leaves where there was expression of either B2 or 2b (see fig. S2). We further demonstrated that B2 was able to functionally substitute for 2b of cucumber mosaic virus (CMV) in whole plant infections (see methods sections of online ma-

Department of Plant Pathology and Center for Plant Cell Biology, University of California, Riverside, CA 92521, USA.

*To whom correspondence should be addressed. E-mail: shou-wei.ding@ucr.edu